

THE REACTION $^{23}\text{Na}(\alpha, \gamma)^{27}\text{Al}$ (II). Spins, parities and mean lives of ^{27}Al levels

M. J. A. DE VOIGT, J. GROOTENHUIS, J. B. VAN MEURS and C. VAN DER LEUN

Fysisch Laboratorium, Rijksuniversiteit, Utrecht, Nederland

Received 8 May 1971

Abstract: Angular distribution and Doppler-shift attenuation measurements in the reaction $^{23}\text{Na}(\alpha, \gamma)^{27}\text{Al}$ lead to the spin and parity assignments $J^\pi = \frac{7}{2}^+$ to the ^{27}Al $E_x = 4.58$ MeV level, $J^\pi = \frac{5}{2}^+$ to the levels at $E_x = 5.43, 5.67$ and 7.17 MeV, $J^\pi = \frac{1}{2}^+$ to the 6.51 MeV level and $J^\pi = \frac{3}{2}^{(+)}$ to the 7.81 MeV level. The $E_x = 2.69, 2.79$ and 2.81 MeV resonance levels have $J^\pi = \frac{1}{2}^{(+)}, \frac{3}{2}$ and $\frac{1}{2}^+$, respectively. Several quadrupole/dipole amplitude mixing ratios and γ -ray transition strengths are also reported. The combined evidence of the decay of the resonance levels and bound states leads to lower limits of $\frac{7}{2}, \frac{5}{2}, \frac{3}{2}, \frac{3}{2}$ and $\frac{7}{2}$ for the spins of the $5.50, 5.96, 6.95, 7.44$ and 7.66 MeV levels, respectively, and to similar spin limitations for seventeen resonances.

Mean lives of the $3.00, 4.51, 4.58, 5.43, 5.67, 5.96, 6.51, 7.66$ and 7.81 MeV levels are $\tau_m = 88 \pm 10, 315 \pm 40, 19 \pm 6, 32 \pm 6, 16 \pm 4, 24 \pm 18, 17 \pm 6, 19 \pm 6$ and 26 ± 6 fs, respectively. Upper limits are given for the mean lives of fourteen other bound states. Eight of these follow from additional $^{26}\text{Mg}(p, \gamma)^{27}\text{Al}$ Doppler-shift attenuation measurements.

E

NUCLEAR REACTIONS $^{23}\text{N}(\alpha, \gamma), E = 2.0\text{--}3.3$ MeV; measured $\sigma(E_\gamma, \theta), E_\gamma(\theta)$.
 $^{26}\text{Mg}(p, \gamma), E = 2.0\text{--}3.0$ MeV; measured $E_\gamma(\theta)$. ^{27}Al levels deduced $J, \pi, \delta, \tau_m, \Gamma_\gamma$.
 Natural Na target, enriched ^{26}Mg target.

1. Introduction

A large number of spins and parities of bound nuclear states has been assigned previously on the basis of angular distribution or correlation measurements in capture reactions. This number can usually be enlarged when the lifetimes of the levels studied are also known. Therefore, a combination of angular distribution and Doppler-shift attenuation (DSA) measurements is often fruitful. This paper describes measurements of this type on the $^{23}\text{Na}(\alpha, \gamma)^{27}\text{Al}$ reaction, which lead to unique spin assignments to six bound states and to three resonance levels of ^{27}Al , and to seven unique even parities. The multipole mixing ratios and transition strengths of many γ -rays in the decay of ^{27}Al are also reported. The decay schemes of twenty $^{23}\text{Na}(\alpha, \gamma)$ resonances, which form a basis for the present investigation, are reported in ref. ¹⁾ hereafter referred to as paper I.

To check the influence of the initial velocity of the recoiling ^{27}Al ions and of the mass of the stopping material on the deduced mean lives, additional DSA measurements with the reaction $^{26}\text{Mg}(p, \gamma)^{27}\text{Al}$ were performed.

2. Lifetime measurements

Mean lives of the lowest twelve excited states of ^{27}Al (up to 4.58 MeV) have been reported previously (2^{-5}). The (α, γ) reaction is attractive for DSA measurements since the complication of coincidence measurements is avoided in capture reactions and because of the relatively high initial velocity of the recoiling ^{27}Al ions, which amounts to $v/c = 0.006$ at $E_\alpha = 3$ MeV. The Ge(Li) detectors enable the accurate determination of the corresponding shifts, which amount up to $\Delta E_\gamma/E_\gamma \approx 0.01$ in the present investigation.

The main problem in the application of the DSA method is the insufficient knowledge of the slowing-down process. Especially at low initial velocities and for stopping in heavy materials, difficulties may arise in the analysis due to the dominating and insufficiently known nuclear part of the stopping power. From detailed measurements Currie *et al.* ⁶⁾ conclude that for stopping in heavy material the usual analysis leads to shorter mean lives than for stopping in lighter material.

The present experiments were carried out at ten $^{23}\text{Na}(\alpha, \gamma)^{27}\text{Al}$ resonances which strongly excite the bound states of interest.

2.1. EXPERIMENTAL PROCEDURE

The apparatus has been described in detail in paper I. Gamma-ray spectra were measured with a Ge(Li) detector at $\theta = 0^\circ$ and 135° and stored in two groups of 2048 channels of a pulse-height analyser. The distance D between target and detector (front face) was $D \approx 3.5$ cm. The measurements at the two angles were carried out in many short (20 min) runs as a precaution against a systematic influence of gain drifts. The target room was temperature controlled, but no special gain stabilization was used. A check on the reliability is the observation of non-shifted γ -rays from long-lived levels, and of fully shifted γ -rays from short-lived resonance levels. An illustrative example of the $^{23}\text{Na}(\alpha, \gamma)$ DSA measurements is given in fig. 1, and of the $^{26}\text{Mg}(p, \gamma)$ measurements in fig. 2.

Peak positions in the γ -ray spectra were determined by first-moment calculations. Solid-angle corrections have been applied, amounting to a reduction of about 2% of the full shifts. All primary γ -rays exhibit full shifts within the experimental errors (see figs. 1 and 2).

To reduce systematic errors due to the uncertainties in the stopping power, NaCl and Na_2WO_4 targets of various thicknesses evaporated onto a directly water cooled 0.5 mm thick copper backing have been used. The thicknesses varied between 5 and $200 \mu\text{g}/\text{cm}^2$, resulting in different contributions of the backing material to the slowing-down process. From resonance strength measurements (see paper I), it was found that the molecular composition of the target did not change drastically during or after the evaporation.

In the $^{26}\text{Mg}(p, \gamma)$ measurements the MgO targets, enriched to 99% in ^{26}Mg , evaporated onto sodium-free 0.3 mm thick tantalum backings, were obtained from

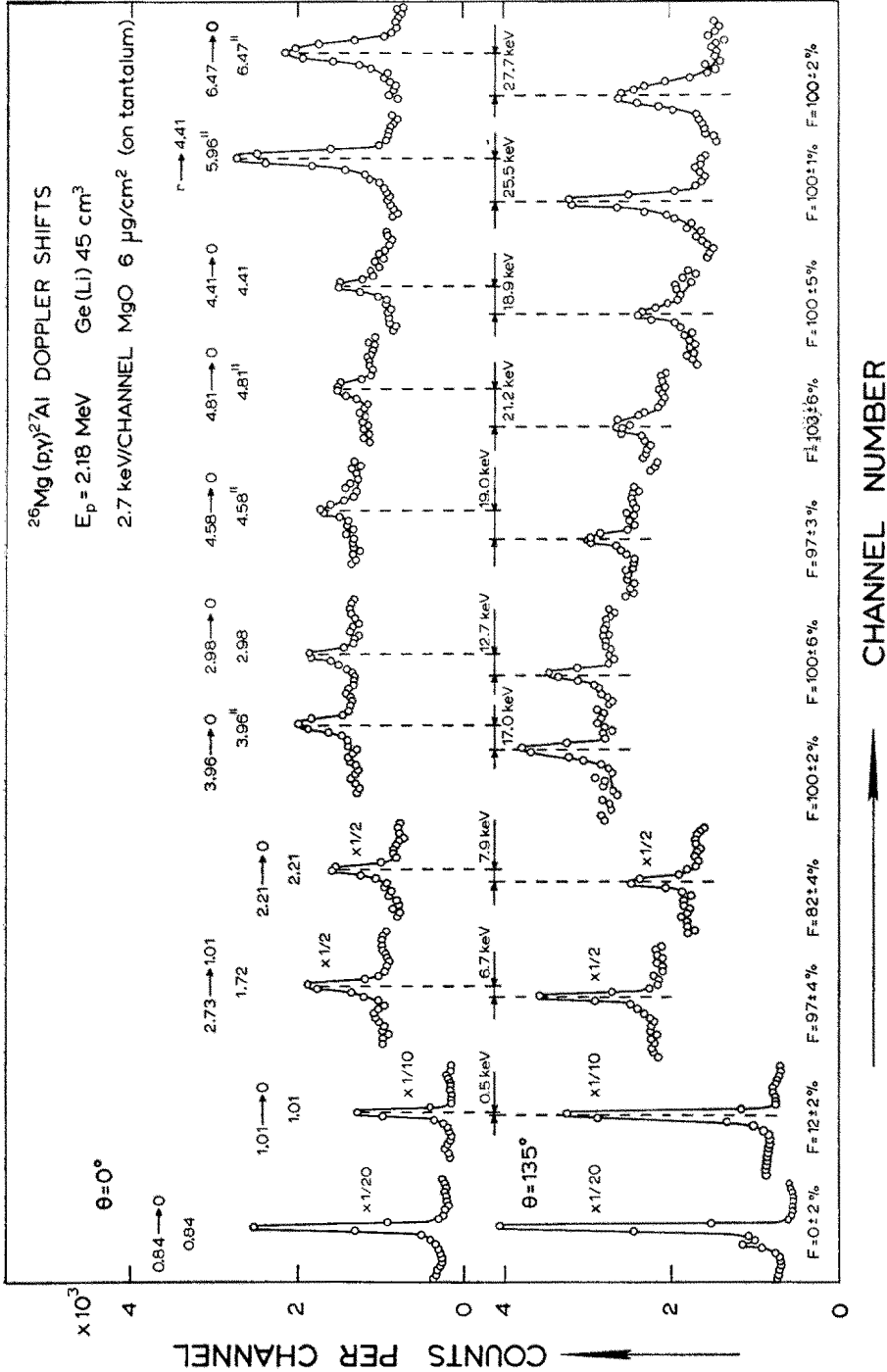


Fig. 2. Doppler shifts measured at $E = 2.18 \text{ MeV}$ $^{26}\text{Mg}(p, \gamma)^{27}\text{Al}$ resonance. For the primary γ -rays which are not indicated, full shifts have been measured within the experimental errors ($r \rightarrow 3.96 \text{ MeV}$, $F = 100 \pm 2\%$, $r \rightarrow 4.58 \text{ MeV}$, $F = 101 \pm 3\%$, $r \rightarrow 6.47 \text{ MeV}$, $F = 99 \pm 3\%$). For other details see caption of fig. 1.

AERE, Harwell (England). Different targets with thicknesses between 5 and 10 $\mu\text{g}/\text{cm}^2$ have been used. The recoiling ^{27}Al ions were stopped mainly in the tantalum backing.

2.2. STOPPING POWERS AND $F(\tau_m)$ CURVES

The fraction $F(\tau_m)$ of the full Doppler shift as a function of the mean life τ_m of the γ -ray emitting nuclear level has been calculated with the slowing-down theory developed by Lindhard *et al.*⁷⁾. Large-angle scattering has been taken into account

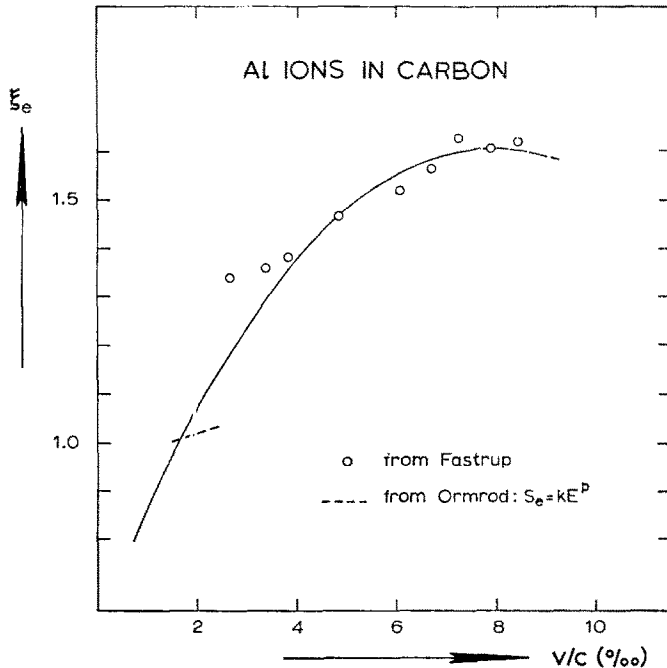


Fig. 3. The velocity dependence of ξ_e , as defined in ref. ¹⁰⁾, for ^{27}Al ions in carbon as extracted from the experimental data ^{10,11)}. The theoretical estimate ⁷⁾ for ξ_e is $\xi_e = Z^{\frac{1}{2}} = 1.53$.

following the method of Blaugrund⁸⁾. It has been pointed out by Engelbertink and Van Middelkoop⁹⁾ that the velocity dependence of the electronic loss function S_e can be calculated from the experimental information of Fastrup *et al.*¹⁰⁾ and Ormrod *et al.*¹¹⁾. From S_e the quantity ξ_e , as defined in ref. ¹⁰⁾, can be calculated in the range $v/c = 0.001-0.009$ for ^{27}Al ions slowing down in carbon. As the experimental errors in the data of Fastrup and of Ormrod are very similar ($\approx 10\%$) it is reasonable to take into account both data by a quadratic fit yielding $\xi_e = 0.627 + 2.493 v/c - 1.577 (v/c)^2$. Here v/c is expressed in $\%$. This function is given in fig. 3 together with the experimental data. From these ξ_e values, which are considered¹¹⁾ to be independent of the atomic number of the stopping material, one can calculate S_e for any stopping material. The stopping powers, calculated in this way agree within the combined experimental errors with those collected by Northcliffe and Schilling¹²⁾.

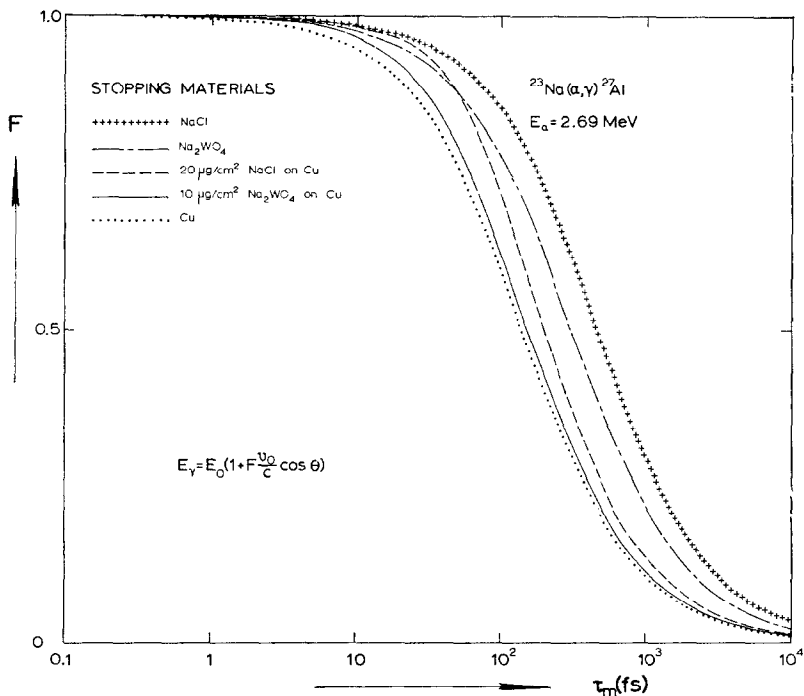


Fig. 4. The Doppler shifts expressed as a fraction F of the full shift, as a function of the mean life τ_m , computed from the slowing-down theory discussed in subject. 2.2. The curves are given for several combinations of target and backing materials used in the $^{23}\text{Na}(\alpha, \gamma)^{27}\text{Al}$ reaction.

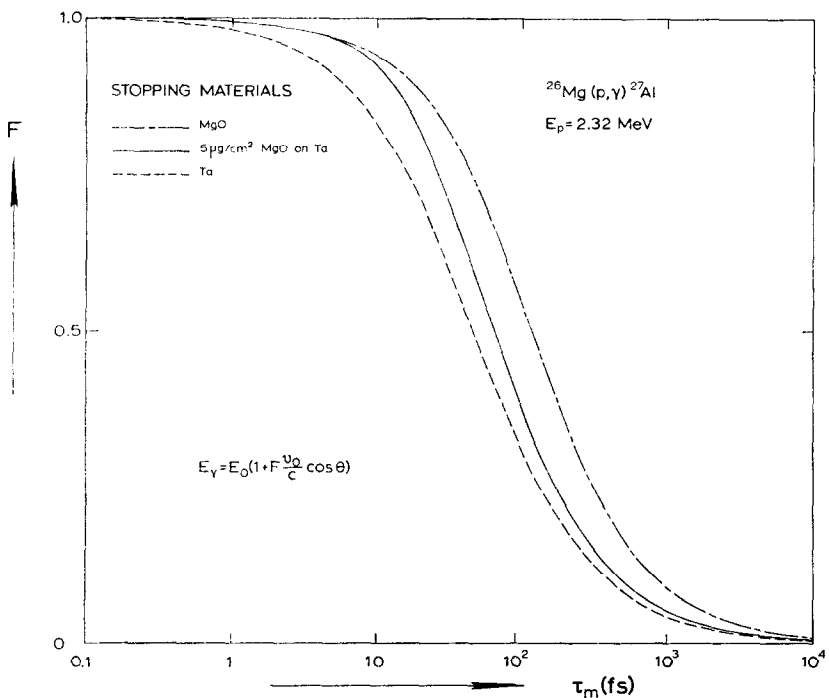


Fig. 5. The $F(\tau_m)$ curves for the slowing-down of ^{27}Al ions in the target and backing material and for the combination of the two, used in the $^{26}\text{Mg}(p, \gamma)^{27}\text{Al}$ reaction.

The $F(\tau_m)$ curves calculated with a computer program are given for the (α, γ) reaction in fig. 4 and for the (p, γ) reaction in fig. 5. The contributions of target and backing material to the DSA have been taken into account.

Most of the levels in question are excited directly from the resonance. The mean lives of the resonance levels, all < 1 fs, could be neglected. Corrections have been applied for levels which are also partly excited in a cascade through a higher level with a non-negligible mean life.

2.3. ERRORS ASSIGNED TO THE MEAN LIVES

The variations in the stopping powers and the ensuing changes in the deduced mean lives are of the same order in the range $F = 10$ – 90 %. The stopping powers used in the analysis of the (α, γ) data are believed to be accurate to about 20 %. The systematic errors in the mean lives deduced from the (α, γ) reaction are mainly composed of the following sources of errors.

- (i) An error of 10–20 %, depending on the number of different (combinations of) stopping materials, due to the uncertainties in the stopping powers.
- (ii) An error of 3–10 %, depending on the number of measurements with different targets, due to the uncertainties in the target thicknesses.

The quoted errors in the mean lives result from a quadratic addition of the statistical errors, which are directly related to the standard deviations in F , and the systematic errors mentioned above. For the errors in the data deduced from the $^{26}\text{Mg}(p, \gamma)$ measurements, see subsect. 2.4.

2.4. RESULTS

As an example, the results of twelve $^{23}\text{Na}(\alpha, \gamma)$ lifetime measurements for the 3.00 MeV level of ^{27}Al are given in table 1. The final result is obtained from the average of the individual F -values which were transposed to the $F(\tau_m)$ curve given in fig. 4 corresponding to $10 \mu\text{g}/\text{cm}^2 \text{Na}_2\text{WO}_4$ on Cu. The small deviations of the individual values from the average mean life demonstrate the reliability of the interpretation of the slowing-down process for the different stopping materials used here.

For the other levels the same procedure has been followed. For each level the number of independent measurements is given in table 2, together with the averaged results and with previously published data.

The final results of the $^{26}\text{Mg}(p, \gamma)$ measurements are obtained from the average of the individual F -values which were transposed to the $F(\tau_m)$ curve given in fig. 5 corresponding to $5 \mu\text{g}/\text{cm}^2 \text{MgO}$ on Ta. The Doppler shifts for the γ -rays de-exciting the 1.01, 2.21 and 3.00 MeV levels are attenuated to $F = 8.2 \pm 1.0$, 87 ± 2 and 63 ± 3 % of the full shifts, respectively. The mean lives deduced as discussed above, and compared with previous data are 600 ± 300 fs (1500 ± 600 fs [refs. ^{2, 3}]), 20 ± 10 fs (41 ± 2 fs [refs. ^{2, 5}]) and 45 ± 15 fs (80 ± 15 fs [refs. ^{2, 5}]) and 88 ± 10 fs [table 2]. These three mean lives are about a factor of two below the literature values. This large discrepancy is most probably due to the low initial velocity of the recoiling ions ($v/c \approx$

TABLE 1
Mean life of the $E_x = 3.00$ MeV level

E_x (MeV)	Target	$F^a)$ (%)	τ_m (fs)
2.40	40 $\mu\text{g}/\text{cm}^2$ NaCl on Cu	82 ± 4	86 ± 15
2.42	12 $\mu\text{g}/\text{cm}^2$ NaCl on Cu	65 ± 4	104 ± 15
2.69	9 $\mu\text{g}/\text{cm}^2$ Na ₂ WO ₄ on Cu	64 ± 6	95 ± 22
2.69	11 $\mu\text{g}/\text{cm}^2$ Na ₂ WO ₄ on Cu	65 ± 6	92 ± 22
2.69	20 $\mu\text{g}/\text{cm}^2$ NaCl on Cu	77 ± 9	82 ± 28
2.69	200 $\mu\text{g}/\text{cm}^2$ NaCl on Cu	90 ± 4	82 ± 18
2.69	10 $\mu\text{g}/\text{cm}^2$ NaCl on Ta	75 ± 8	60 ± 18
2.81	5 $\mu\text{g}/\text{cm}^2$ Na ₂ WO ₄ on Cu	71 ± 18	70 ± 60
2.81	15 $\mu\text{g}/\text{cm}^2$ NaCl on Cu	72 ± 4	92 ± 15
2.86	12 $\mu\text{g}/\text{cm}^2$ Na ₂ WO ₄ on Cu	66 ± 4	88 ± 12
2.86	10 $\mu\text{g}/\text{cm}^2$ NaCl on Cu	71 ± 4	85 ± 15
2.94	13 $\mu\text{g}/\text{cm}^2$ Na ₂ WO ₄ on Cu	74 ± 10	70 ± 30
		average value	$88 \pm 6^b)$

^{a)} Corrected for indirect excitation.

^{b)} From the average of the individual F -values, which were transposed to the $F(\tau_m)$ curve given in fig. 4 (10 $\mu\text{g}/\text{cm}^2$ Na₂WO₄ on Cu). The error represents the statistical error only.

TABLE 2
Mean lives of ^{27}Al states measured with the $^{23}\text{Na}(\alpha, \gamma)^{27}\text{Al}$ reaction

$E_x^a)$ (MeV)	Present experiment			$\tau_m^c)$ (fs)	Previous work τ_m (fs)
	number of measurements	$F^b)$ (%)			
3.00	12	65 ± 2		88 ± 10	$80 \pm 15^d)$
4.51	9	31.0 ± 1.3		315 ± 40	$320 \pm 35^e)$
4.58	7	93 ± 3		19 ± 6	$\leq 30^f)$
4.81	1	98 ± 8		≤ 30	
5.43	10	87 ± 2		32 ± 6	
5.50	8	99.0 ± 1.5		≤ 10	
5.67	12	94.0 ± 1.3		16 ± 4	
5.96	2	90 ± 6		24 ± 18	
6.48	2	99 ± 4		≤ 20	
6.51	4	94 ± 3		17 ± 6	
6.95	3	98 ± 4		≤ 20	
7.17	6	100 ± 2		≤ 10	
7.44	4	100 ± 2		≤ 10	
7.66	4	93 ± 3		19 ± 6	
7.81	5	89 ± 2		26 ± 6	

^{a)} From $^{26}\text{Mg}(p, \gamma)^{27}\text{Al}$ DSA measurements the mean lives of the 2.73, 2.98, 3.68, 3.96, 4.05, 4.41, 4.58, 5.55, 6.47 and 6.48 MeV levels are limited to $\tau_m \leq 25$ fs (see subsect. 2.4).

^{b)} Averages of the individual F -values, which were transposed to the $F(\tau_m)$ curve given in fig. 4 (10 $\mu\text{g}/\text{cm}^2$ Na₂WO₄ on Cu).

^{c)} The errors include the statistical and systematic errors (see subsect. 2.3).

^{d)} Average value from refs. 2, 5).

^{e)} Average value from refs. 3, 4). An extra error of 15% has been added before averaging to take into account the uncertainties in the stopping powers.

^{f)} Ref. 3).

0.002) and to the heavy slowing-down material (tantalum). The present discrepancies between mean lives deduced with light and heavy stopping materials agree with those found by Currie *et al.*^{6, 13}).

The (p, γ) measurements of very short mean lives are expected to be less affected by these difficulties since then the slowing down takes place mainly in the lighter target material. For the 2.73, 2.98, 3.68, 3.96, 4.05, 4.41, 4.58, 5.55, 6.47 and 6.48 MeV levels the Doppler shifts, as found in several independent measurements, are all larger than 92 % of the full shifts. Including an extra error of 50 % due to the uncertainties in the stopping powers this leads to an upper limit $\tau_m \leq 25$ fs for the 10 levels mentioned above. These limits agree with previously reported^{2, 3, 5}) mean lives of seven levels.

3. Spin and parity determinations

The strongest four resonances which decay through previously not reported bound states in ^{27}Al (see paper I) have been selected for angular distribution measurements. Selection was imperative because of the long measuring times (see below).

Resonance spins were deduced from angular distributions of primary γ -rays to the 2.21, 3.00 and 4.51 MeV levels. The spins and parities of the first two levels are known to be $J^\pi = \frac{7}{2}^+$ and $\frac{9}{2}^+$, respectively¹⁴). From a $^{24}\text{Mg}(\alpha, p\gamma)^{27}\text{Al}$ angular correlation experiment¹⁵) and the mean life $\tau_m = 320 \pm 35$ fs [refs. ^{3, 4})], it follows that $J^\pi(4.51) = \frac{11}{2}^+$.

3.1. EXPERIMENTAL PROCEDURE

Gamma-rays were measured with a Ge(Li) detector at $\theta = 0^\circ, 35^\circ, 55^\circ$ and 90° at $D = 3$ cm, while a NaI scintillator served as a monitor. The Ge(Li) spectra were recorded in four 1024-channel memory sections of a 4096-channel LABEN analyser. Every 20 min the detector position was changed as a precaution against systematic errors due to target deterioration and drifts of the electronics. The eccentricity of the target spot was checked with the same target at the $E_p = 512$ keV $^{23}\text{Na}(p, \gamma)^{24}\text{Mg}$ resonance where the strong $E_\gamma = 10.81$ MeV primary γ -rays ($r \rightarrow 1.37$ MeV) are isotropic. The measured¹⁶) Legendre polynomial coefficients are $A_2 = +0.001 \pm 0.005$ and $A_4 = -0.008 \pm 0.005$. Corrections have been applied for the measured eccentricity and for the difference in γ -ray absorption in the target holder at the four angles. The beam current was 10–15 μA . At the $E_\alpha = 2.69$ and 2.81 MeV resonances the data of two three-day runs were added to obtain sufficient statistics. At each of the $E_\alpha = 2.79$ and 3.14 MeV resonances the measuring time was about three days.

3.2. ANALYSIS

The theoretical description of the $^{23}\text{Na}(\alpha, \gamma)$ angular distributions is simple, because the α -particle is spinless. The theory has been treated extensively in several publications^{17, 18}).

For high-spin resonance levels the anisotropy is practically independent of the relative population of the $|m| = \frac{1}{2}$ and $|m| = \frac{3}{2}$ magnetic substates (the ^{23}Na ground state has $J^\pi = \frac{3}{2}^+$). The influence of the population parameters $p(m)$ on the angular distributions has been investigated. A typical example of a least-squares fit of a theoretical angular distribution to the experimental data, as a function of the quadrupole/dipole amplitude mixing ratio x with $p(\frac{1}{2})$ fixed as well as variable is

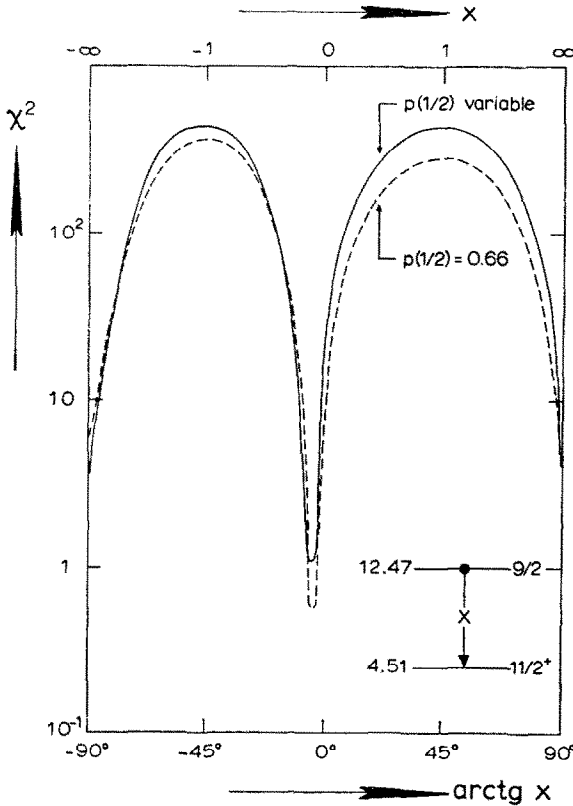


Fig. 6. The normalized χ^2 curve for the angular distribution of the 12.47 \rightarrow 4.51 MeV transition at the $E_\alpha = 2.79$ MeV $^{23}\text{Na}(\alpha, \gamma)^{27}\text{Al}$ resonance. The values of χ^2 are plotted against the quadrupole/dipole amplitude mixing ratio with fixed and variable population parameters. The differences in χ^2 are mainly due to the different number of degrees of freedom (2 and 1, respectively).

given in fig. 6. There is no significant difference between the two curves. On this basis it was concluded that an arbitrary value of $p(m)$ could be chosen in the analysis.

From the calculated penetration factors for 3 MeV α -particles in the ^{23}Na nucleus, $l_\alpha = 6$ capture was found to be about a factor of 100 less probable than $l_\alpha = 4$ capture in the formation of $J^\pi = \frac{9}{2}^+$ and $\frac{11}{2}^+$ resonances. If the orbital momentum of the α -particles is taken to be minimal it is possible to calculate $p(m)$ from Clebsch-Gordan coefficients; one finds $p(\frac{1}{2}) = 0.68, 0.66$ and 0.64 for $J_r = \frac{1}{2}^-, \frac{3}{2}^-$ and $\frac{7}{2}^-$,

These results and the ensuing mixing ratios (see table 3) generally agree well with those of Röpke and Anyas-Weiss²⁰). They find for the $E_\alpha = 2.69$ MeV resonance $J_r^\pi = \frac{1}{2}^-$ or $\frac{3}{2}^+$, and (for $J_r = \frac{1}{2}^-$) $x = 0.00 \pm 0.10$, -0.1 ± 0.3 and 0.13 ± 0.09 for the $r \rightarrow 3.00$, $r \rightarrow 4.51$ and $r \rightarrow 5.67$ MeV transitions, respectively. At $E_\alpha = 2.79$ MeV;

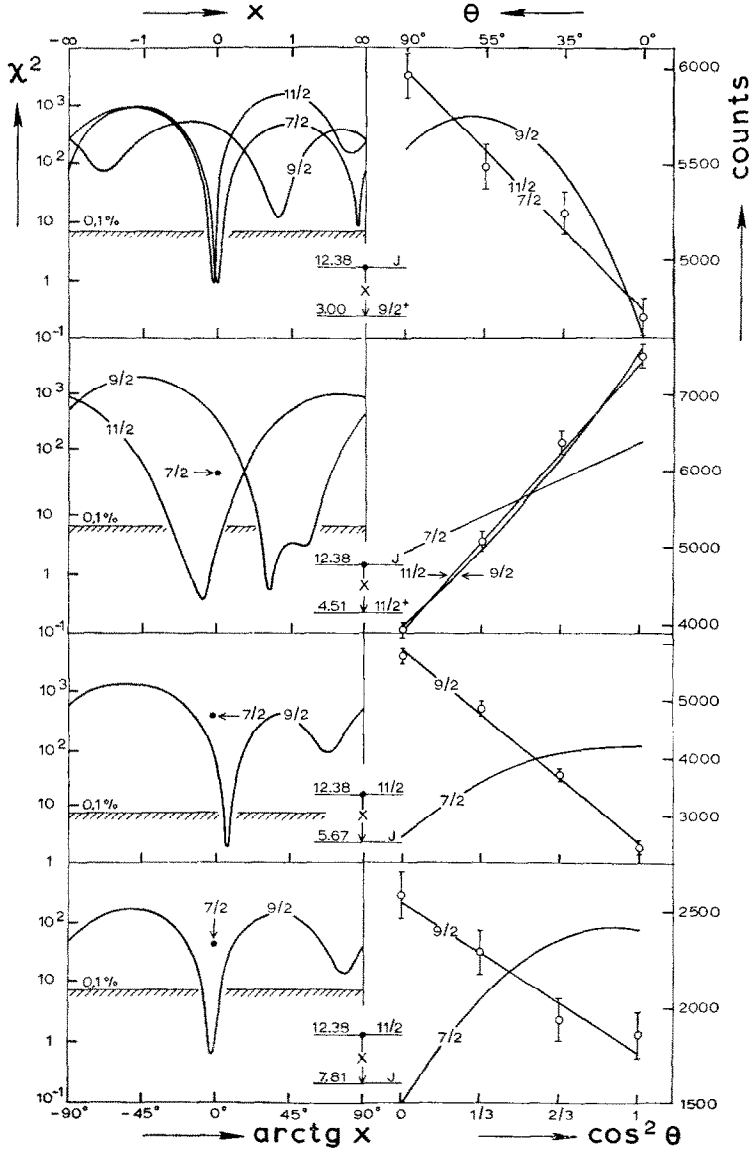


Fig. 7. The angular distribution data with theoretical fits and corresponding χ^2 curves at the $E_\alpha = 2.69$ MeV $^{23}\text{Na}(\alpha, \gamma)^{27}\text{Al}$ resonance. The values of χ^2 are plotted against the amplitude mixing ratios with J as a parameter. The measurement uniquely determines the resonance spin as $J = \frac{1}{2}^-$ and, in addition, the spins of the 5.67 and 7.81 MeV levels as $J = \frac{3}{2}^-$.

respectively. These values were used in the analysis. Correction factors $Q_2 = 0.91$ and $Q_4 = 0.74$ [ref. ¹⁹)] for the finite solid angle of the detector have been taken into account.

The data were fitted to theoretical angular distributions for all possible spin combinations. The number of combinations was limited by discarding pure octupole character for observed γ -ray transitions. This procedure is justified since even the weakest observed transitions would have, if E3 character is assumed, strengths of more than 50 W.u.

The least-squares method as described in ref. ¹⁴) has been applied in the angular distribution fitting. An ALGOL computer program calculates the value of χ^2 as a function of $\text{arctg } x$. Here χ^2 is the normalized value of Q^2 ; $\chi^2 = Q^2/n$, where n is the number of degrees of freedom. For the mixing ratios x the phase convention of Smith ¹⁸) has been used. The values of $\text{arctg } x$ were varied in steps of 2° from -90° to $+90^\circ$. The best values of $\text{arctg } x$ were found by means of an iteration procedure which fitted the χ^2 curve with a parabola in the region of the minimum. For unambiguous spin determinations the 99.9% confidence criterium has been applied. The error in the mixing ratio, corresponding to the statistical standard deviation, is found by intersecting the (unnormalized) Q^2 function with the line $Q^2 = Q_{\min}^2 + 1$. If χ_{\min}^2 is larger than unity the error in $\text{arctg } x$ is multiplied by $\sqrt{\chi_{\min}^2}$.

Parities have been obtained by discarding M2 character for observed γ -ray transitions with strengths larger than 5 W.u. Parities are given in brackets if the opposite parity leads to an M2 strength between 1 and 5 W.u. These strengths can be calculated from the resonance strengths, branching ratios, mixing ratios and mean lives of bound states.

3.3. RESULTS

The angular distribution data and the results of the χ^2 analyses are presented in figs. 7, 8 and 9. A summary of measured quadrupole/dipole mixing ratios, level widths and transition strengths is given in table 3. A short discussion of the conclusions drawn from the data is given below. The numerical data used in this discussion are given in the tables 2 and 3 of this paper and in figs. 8 and 9 of paper I.

3.3.1. Resonance levels

The $E_\alpha = 2.69, 2.79$ and 2.81 MeV resonance levels. On the basis of the decay schemes the possible values are limited to $J = \frac{7}{2}, \frac{9}{2}$ and $\frac{11}{2}$ for the $E_\alpha = 2.69$ and 2.79 MeV resonance levels and to $J = \frac{5}{2}$ through $\frac{11}{2}$ for the $E_\alpha = 2.81$ MeV resonance level. Least-squares fits of the angular distributions of the primary γ -rays uniquely yield $J_r = \frac{11}{2}, \frac{9}{2}$ and $\frac{11}{2}$ for the $E_\alpha = 2.69, 2.79$ and 2.81 MeV resonances, respectively (see figs. 7, 8 and 9). Assumed odd parities lead to M2 admixtures larger than 2.0 W.u. in the $r \rightarrow 5.67$ MeV ($\frac{9}{2}^+$) transition at the $E_\alpha = 2.69$ MeV resonance and larger than 90 W.u. in the $r \rightarrow 6.51$ MeV ($\frac{11}{2}^+$) transition at the $E_\alpha = 2.81$ MeV resonance. *Conclusions:* $J_r^\pi = \frac{11}{2}^+, \frac{9}{2}$ and $\frac{11}{2}^+$ for the $E_\alpha = 2.69, 2.79$ and 2.81 MeV resonance levels, respectively.

$J^\pi = \frac{9}{2}^+$ and $x = -0.04 \pm 0.08$ for the $r \rightarrow 2.21$ MeV transition. The discrepancies with ref. ²⁰⁾ for the mixing ratios of the $r \rightarrow 4.51$ and $r \rightarrow 4.58$ MeV transitions at the $E_\alpha = 2.79$ MeV resonance may be due to an underestimate of the systematic errors in ref. ²⁰⁾.

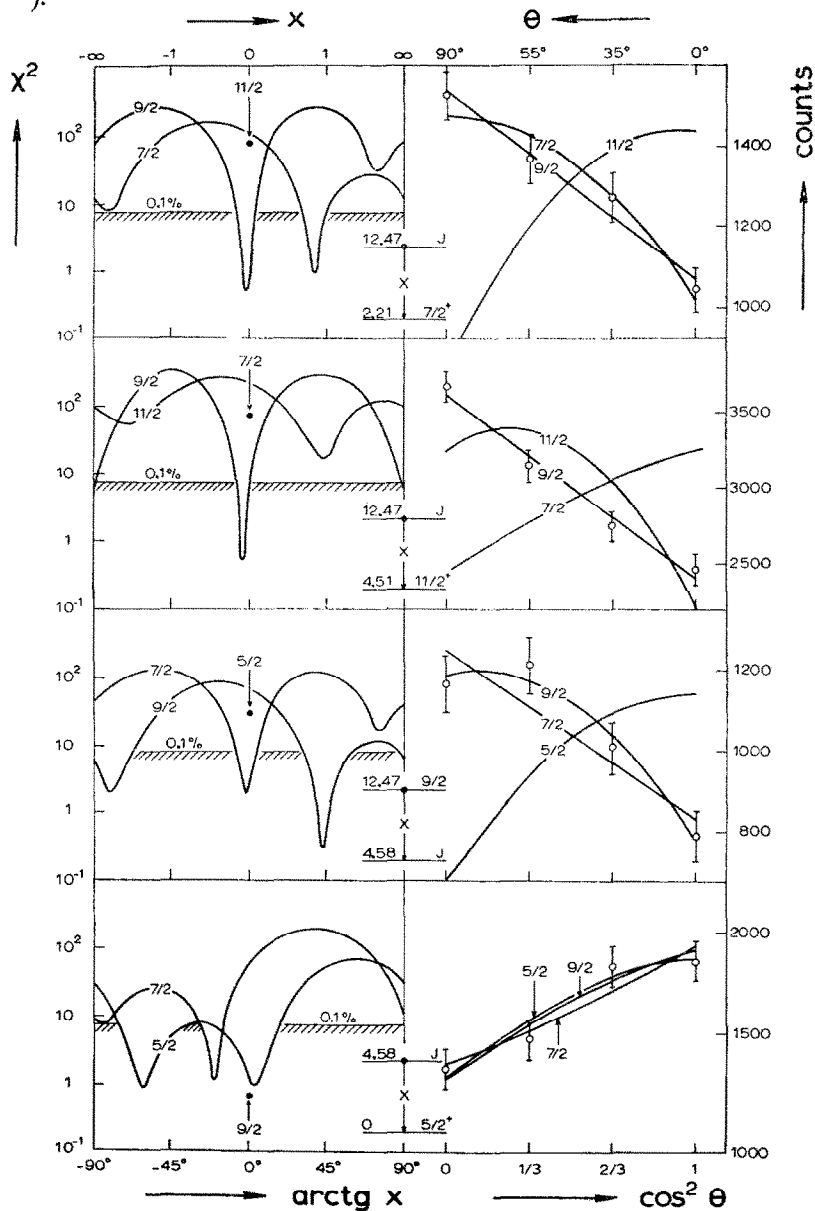


Fig. 8. The angular distribution data with theoretical fits and the corresponding χ^2 curves at the $E_\alpha = 2.79$ MeV $^{23}\text{Na}(\alpha, \gamma)^{27}\text{Al}$ resonance. The measurement uniquely determines the resonance spin as $J = \frac{9}{2}$ and, in addition, it restricts the spin of the 4.58 MeV level to $J = (\frac{7}{2}, \frac{5}{2})$.

The $E_\alpha = 3.14$ MeV resonance level. Due to high background it was only possible to restrict the resonance spin to $\frac{9}{2}$ or $\frac{7}{2}$ on the basis of the angular distribution of the primary γ -rays to the $E_x = 5.50$ MeV ($J^\pi \cong \frac{7}{2}^+$) level. The parity is probably even since odd parity would lead to M2 strengths above 1 W.u. for the $r \rightarrow 2.21$ ($\frac{7}{2}^+$) and $r \rightarrow 5.43$ MeV ($\frac{9}{2}^+$) transitions. *Conclusion:* $J_r^\pi = (\frac{7}{2}^+, \frac{9}{2}^+)$.

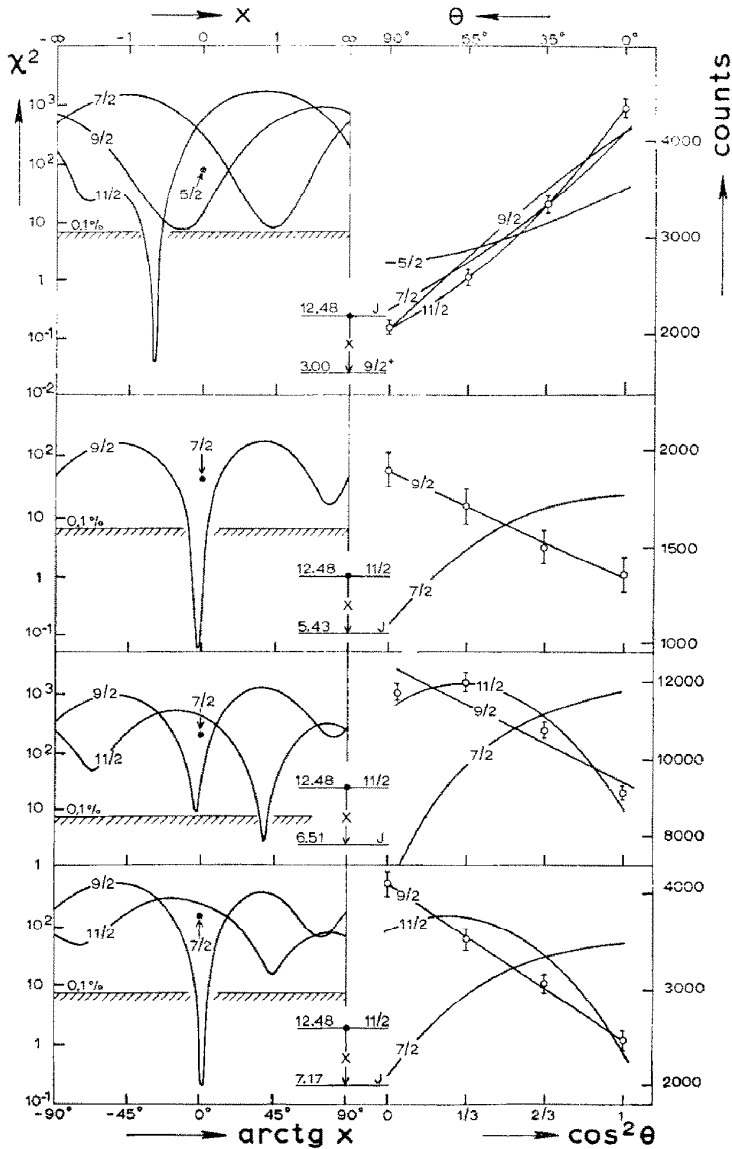


Fig. 9. The angular distribution data with theoretical fits and corresponding χ^2 curves at the $E_\alpha = 2.81$ MeV $^{23}\text{Na}(\alpha, \gamma)^{27}\text{Al}$ resonance. The measurement uniquely determines the resonance spin as $J = \frac{7}{2}$ and, in addition, yields $J = \frac{9}{2}$, $\frac{11}{2}$ and $\frac{9}{2}$ for the $E_x = 5.43$, 6.51 and 7.17 MeV levels respectively.

TABLE 3

Quadrupole/dipole amplitude mixing ratios, radiative widths and strengths in W.u. of γ -ray transitions in ^{27}Al

E_α ^{a)} (MeV)	Transition (E_x in MeV)	$J_1^\pi \rightarrow J_2^\pi$	Mixing ratio x	Γ_γ ^{b)} (meV)	$ M(M1) ^2$ ^{c)} $\times 10^2$	$ M(E2) ^2$ ^{c)}
Resonance levels						
2.69	12.38 \rightarrow 3.00	$\frac{1}{2}^+(+) \rightarrow \frac{3}{2}^+$	-0.070 ± 0.009	> 190	> 1	> 0.003
	12.38 \rightarrow 4.51	$\frac{1}{2}^+(+) \rightarrow \frac{1}{2}^+$	-0.13 ± 0.09	> 140	> 1	> 0.009
	12.38 \rightarrow 5.67	$\frac{1}{2}^+(+) \rightarrow \frac{3}{2}^+$	$+0.118 \pm 0.013$	> 260	> 4	> 0.07
	12.38 \rightarrow 7.81	$\frac{1}{2}^+(+) \rightarrow \frac{3}{2}^+(+)$	-0.03 ± 0.03	> 100	> 5	
2.79	12.47 \rightarrow 2.21	$\frac{3}{2}^+ \rightarrow \frac{3}{2}^+$	-0.042 ± 0.019	> 170	(> 0.8)	> 0.0005
	12.47 \rightarrow 3.00	$\frac{3}{2}^+ \rightarrow \frac{3}{2}^+$	-0.7 ± 0.6	> 20	(> 0.06)	> 0.003
	12.47 \rightarrow 4.51	$\frac{3}{2}^+ \rightarrow \frac{1}{2}^+$	-0.07 ± 0.02	> 320	(> 3)	> 0.01
	12.47 \rightarrow 4.58	$\frac{3}{2}^+ \rightarrow \frac{7}{2}^+$	-0.02 ± 0.04	> 110	(> 1)	
2.81	12.48 \rightarrow 2.21	$\frac{1}{2}^+ \rightarrow \frac{3}{2}^+$	∞	> 40		> 0.09
	12.48 \rightarrow 3.00	$\frac{1}{2}^+ \rightarrow \frac{3}{2}^+$	-0.55 ± 0.04	> 100	> 0.4	> 0.07
	12.48 \rightarrow 5.43	$\frac{1}{2}^+ \rightarrow \frac{3}{2}^+$	-0.04 ± 0.04	> 50	> 0.6	
	12.48 \rightarrow 6.51	$\frac{1}{2}^+ \rightarrow \frac{1}{2}^+$	$+0.82 \pm 0.05$	> 290	> 4	> 3
3.14	12.48 \rightarrow 7.17	$\frac{1}{2}^+ \rightarrow \frac{3}{2}^+$	$+0.02 \pm 0.02$	> 150	> 5	
	12.76 \rightarrow 2.21	$\frac{3}{2}^+(+) \rightarrow \frac{3}{2}^+$	-0.25 ± 0.05	> 30	> 0.1	> 0.004
	12.76 \rightarrow 2.21	$\frac{7}{2}^+(+) \rightarrow \frac{7}{2}^+$	-1.9 ± 0.5	> 40	> 0.05	> 0.05
	12.76 \rightarrow 5.43	$\frac{3}{2}^+(+) \rightarrow \frac{3}{2}^+$	$+0.8 \pm 0.3$	> 15	> 0.1	> 0.06
	12.76 \rightarrow 5.43	$\frac{7}{2}^+(+) \rightarrow \frac{3}{2}^+$	$+0.0 \pm 0.2$	> 20	> 0.2	
Bound states						
2.69	5.67 \rightarrow 0	$\frac{3}{2}^+ \rightarrow \frac{3}{2}^+$	∞	23 ± 5		1.0 ± 0.3
	5.67 \rightarrow 3.00	$\frac{3}{2}^+ \rightarrow \frac{3}{2}^+$	$+0.18 \pm 0.05$	19 ± 5	4.5 ± 1.2	1.1 ± 0.7
	7.81 \rightarrow 0	$\frac{3}{2}^+(+) \rightarrow \frac{3}{2}^+$	∞	5 ± 2		0.04 ± 0.02
	7.81 \rightarrow 2.21	$\frac{3}{2}^+(+) \rightarrow \frac{3}{2}^+$	$+0.12 \pm 0.04$	20 ± 5	0.54 ± 0.13	< 0.02
2.79	4.58 \rightarrow 0	$\frac{7}{2}^+ \rightarrow \frac{3}{2}^+$	-0.35 ± 0.05	27 ± 6	1.2 ± 0.4	0.38 ± 0.13
2.81	5.43 \rightarrow 0	$\frac{3}{2}^+ \rightarrow \frac{3}{2}^+$	∞	8 ± 4		0.44 ± 0.14
	5.43 \rightarrow 2.21	$\frac{3}{2}^+ \rightarrow \frac{7}{2}^+$	$+0.75 \pm 0.13$	12 ± 4	1.2 ± 0.4	3.2 ± 1.1
	6.51 \rightarrow 2.21	$\frac{1}{2}^+ \rightarrow \frac{3}{2}^+$	∞	8 ± 3		1.3 ± 0.6
	6.51 \rightarrow 3.00	$\frac{1}{2}^+ \rightarrow \frac{3}{2}^+$	$+0.33 \pm 0.05$	14 ± 5	1.4 ± 0.6	0.6 ± 0.3
	7.17 \rightarrow 3.00	$\frac{3}{2}^+ \rightarrow \frac{3}{2}^+$	$+0.13 \pm 0.07$	> 35	> 2.8	> 0.14
	7.17 \rightarrow 4.58	$\frac{3}{2}^+ \rightarrow \frac{7}{2}^+$	$+0.24 \pm 0.06$	> 15	> 5.9	> 2.7

^{a)} Alpha particle energy of the resonance at which the transition is observed.

^{b)} For resonances Γ_γ was calculated from the strengths and branching ratios given in paper I and for bound states from the mean lives (see subsect. 2.4) and the branching ratios given in paper I.

^{c)} For transitions between states with unknown parity the strengths are given in brackets.

The $E_\alpha = 2.058, 2.94$ and 3.00 MeV resonance levels. As discussed in paper I the lower member of the $E_\alpha = 2.06$ MeV doublet corresponds to the $J = \frac{1}{2}$ or $\frac{3}{2}$ $^{23}\text{Na}(\alpha, p_0)^{26}\text{Mg}$ resonance ²¹⁾ at $E_\alpha = 2.058$ MeV. The spin assignments to the $E_\alpha = 2.94$ and 3.00 MeV resonance levels are based on the decay scheme only. The spins are given in brackets because the existence of the very weak (3 %) $12.60 \rightarrow 1.01$ MeV ($\frac{3}{2}^+$) and (4 %) $12.64 \rightarrow 6.51$ MeV ($\frac{1}{2}^+$) transitions is not unambiguous. Odd parities would imply M2 strengths larger than 4.5, 0.2, 3.0 and 1.5 W.u. in the primary

γ -ray transitions to the 4.51 and 1.01 MeV levels at the $E_\alpha = 2.94$ MeV resonance, and to the 6.51 and 1.01 MeV levels at the $E_\alpha = 3.00$ MeV resonance, respectively. *Conclusions:* $J_r = \frac{1}{2}$ or $\frac{3}{2}$ for the $E_\alpha = 2.058$ MeV resonance level and $J_r^\pi = (\frac{7}{2}^+)$ for the $E_\alpha = 2.94$ and 3.00 MeV resonance levels.

The spin limitations for the other resonance levels, indicated in fig. 8 of paper I are based on the decay schemes only (see subsect. 3.2).

3.3.2. Bound states

The 5.43, 5.67, 6.51, 7.17 and 7.81 MeV levels. Least-squares fits of the angular distributions of primary γ -rays uniquely determine $J = \frac{1}{2}$ for the 6.51 MeV level (fig. 9) and $J = \frac{9}{2}$ for the four other levels (figs. 7 and 9). The measured mean lives (table 2) for assumed odd parity, would lead to M2 strengths of 13 ± 4 , 29 ± 8 , 39 ± 18 , > 5 and 1.2 ± 0.6 W.u. in the $5.43 \rightarrow 0(\frac{5}{2}^+)$, $5.67 \rightarrow 0$, $6.51 \rightarrow 2.21(\frac{7}{2}^+)$, $7.17 \rightarrow 3.00(\frac{9}{2}^+)$ and $7.81 \rightarrow 0$ MeV transitions, respectively. *Conclusions:* $J^\pi = \frac{9}{2}^+$ for the 5.43, 5.67 and 7.17 MeV levels, $J^\pi(6.51) = \frac{1}{2}^{1+}$ and $J^\pi(7.81) = \frac{9}{2}^{(+)}$.

The previous assignment ²⁰⁾ $J^\pi(5.67) = \frac{9}{2}^+$ or $\frac{7}{2}$ agrees with the present result.

The 4.58 MeV level. A least-squares fit of the angular distributions of the two transitions in the $r \rightarrow 4.58 \rightarrow 0$ MeV cascade at the $E_\alpha = 2.79$ MeV, $J = \frac{9}{2}$ resonance yields $J(4.58) = \frac{7}{2}$ or $\frac{9}{2}$ (fig. 8). Combined with the result of a $^{24}\text{Mg}(\alpha, \text{py})$ angular-correlation experiment ²²⁾, $J(4.58) \leq \frac{7}{2}$, one concludes $J(4.58) = \frac{7}{2}$. The measured mixing ratio for the ground state transition and the mean life would lead, for assumed odd parity, to a strong M2 admixture (12 ± 3 W.u.) in the ground state transition. *Conclusion:* $J^\pi(4.58) = \frac{7}{2}^+$.

The present mixing ratio for the $4.58 \rightarrow 0$ MeV transition, $x = -0.35 \pm 0.05$, agrees well with that of ref. ²⁰⁾, $x = -0.3 \pm 0.2$, but is in disagreement with $x = -0.18 \pm 0.04$ reported in ref. ²²⁾.

The 4.81, 5.50, 5.96, 6.95, 7.44 and 7.66 MeV levels. It is known that the $E_x = 4.81$ MeV state has $J = \frac{5}{2}$ with $x = 0.29 \pm 0.03$ for its ground state transition ¹⁴⁾. From the measured mean life (table 2) then follows $J^\pi(4.81) = \frac{5}{2}^{(+)}$.

The combined evidence of the decay of the resonance levels and bound states, the resonance strengths and the presently determined mean lives yields the following limitations: $J^\pi(5.50) = (\frac{7}{2}, \frac{9}{2}, \frac{1}{2})^+$, $J(5.96) \geq \frac{3}{2}$, $J(6.95) \geq \frac{5}{2}$, $J(7.44) \geq \frac{5}{2}$ and $J(7.66) = (\frac{7}{2}, \frac{9}{2}, \frac{1}{2})$.

4. Radiative widths

From the data given above γ -ray strengths can be deduced. The measured (α, γ) resonance strengths $S = (2J+1)\Gamma_\alpha\Gamma_\gamma/\Gamma$ lead to lower limits for the radiative widths of the resonance levels: $\Gamma_\gamma \geq S/(2J+1)$.

Because of penetration probabilities it is very likely that the relation $\Gamma_p \leq \Gamma_\alpha$ holds for high-spin resonances ($J = \frac{9}{2}$ or $\frac{1}{2}^{1+}$). The same conclusion can be drawn from the absence of corresponding (α, γ) and (α, p) resonances. If the additional (like-

ly) assumption is made that $\Gamma_\gamma \leq \Gamma_\alpha$ one has $\Gamma_\alpha \approx \Gamma$, such that the lower limits of Γ_γ listed in table 3 represent the actual values of Γ_γ .

The radiative widths of the bound states, given in table 3, are calculated from the measured mean lives (table 2), the mixing ratios (table 3) and the branching ratios given in paper I. The transition strengths in W.u., $|M|^2 = \Gamma_\gamma/\Gamma_{\gamma w}$, where $\Gamma_{\gamma w}$ is the Weisskopf estimate²³), are listed in the last two columns of table 3. The strengths of transitions from bound states do not deviate strongly from previously measured transition rates in sd shell nuclei²⁴). If the lower limits of the resonance widths listed in table 3 represent the actual values of Γ_γ , the M1 transitions have normal strengths, but the E2 transitions are relatively weak.

5. Conclusions

The (α, γ) reaction proved to be a useful tool in the selection of high-spin levels. Angular distribution and Doppler-shift (lifetime) measurements lead to unique spin assignments to three resonance levels and six bound states and to seven parities of ^{27}Al levels. The results are summarized in figs. 8 and 9 of paper I. The measured ^{27}Al mean lives are given in table 2.

The combined information on low-spin levels from the $^{26}\text{Mg}(p, \gamma)^{27}\text{Al}$ reaction^{14, 25}), and on high-spin levels from the present work, and investigations of particle reactions^{3, 15, 26}) enables the construction of a rather complete ^{27}Al decay scheme.

The information on odd-parity levels, however, is very scarce. The first unique assignment to an odd-parity level, $J^\pi = \frac{7}{2}^-$ for $E_x = 6.48$ MeV, has only been made recently²⁷).

The high-spin (α, γ) resonances preferentially decay to even-parity levels. This is understandable from the small number of bound states with odd parity and from the relatively large difference (≈ 4 MeV) in the energies of primary γ -rays to even- and odd-parity levels with a high spin. The lowest $J^\pi = \frac{7}{2}^+$ state e.g. is found at 2.21 MeV whereas the lowest $J^\pi = \frac{7}{2}^-$ level has an excitation energy of 6.48 MeV.

Most of the (α, γ) resonances probably have even parity since in the sd shell, γ -ray transitions between levels of opposite parity are rather weak. This phenomenon has been observed both in heavier nuclei (e.g. ^{38}Ar) with pronounced shell structure, as well as in lighter nuclei with rotational-band structure.

It is a pleasure to thank Prof. P. M. Endt for his continuous interest and Dr. G. van Middelkoop for critical reading of the manuscript. This investigation was partly supported by the joint program of the Stichting voor Fundamenteel Onderzoek der Materie and the Nederlandse Organisatie voor Zuiver Wetenschappelijk Onderzoek.

References

- 1) M. J. A. de Voigt, J. W. Maas, D. Veenhof and C. van der Leun, Nucl. Phys. **A170** (1971) 448
- 2) P. M. Endt and C. van der Leun, Nucl. Phys. **A105** (1967) 1
- 3) P. J. M. Smulders, C. Broude and J. F. Sharpey-Schafer, Can. J. Phys. **46** (1968) 261

- 4) H. Röpke and S. T. Lam, *Can. J. Phys.* **46** (1968) 1649
- 5) S. W. Robinson, C. P. Swann and V. K. Rasmussen, *Phys. Rev.* **174** (1968) 1320
- 6) W. M. Currie, J. G. Earwaker and J. Martin, *Nucl. Phys.* **A135** (1969) 325
- 7) J. Lindhard, M. Scharff and G. E. Schiøtt, *Mat. Fys. Medd. Dan. Vid. Selsk.* **33** (1963) no. 14
- 8) A. E. Blaugrund, *Nucl. Phys.* **88** (1966) 501
- 9) G. A. P. Engelbertink and G. van Middelkoop, *Nucl. Phys.* **A138** (1969) 588;
G. van Middelkoop and G. A. P. Engelbertink, *Nucl. Phys.* **A138** (1969) 601;
G. van Middelkoop and C. J. Th. Gusing, *Nucl. Phys.* **A147** (1970) 225
- 10) B. Fastrup, P. Hvelplund and C. A. Sauter, *Mat. Fys. Medd. Dan. Vid. Selsk.* **35** (1966) no. 10
- 11) J. H. Ormrod, J. R. MacDonald and H. E. Duckworth, *Can. J. Phys.* **43** (1965) 275
- 12) L. C. Northcliffe and R. F. Schilling, *Nucl. Data A7* (1970) 233
- 13) W. M. Currie, *Nucl. Instr.* **73** (1969) 173
- 14) D. M. Sheppard and C. van der Leun, *Nucl. Phys.* **A100** (1967) 333
- 15) K. W. Carter, D. C. Kean, C. J. Pifuso and R. H. Spear, *Nucl. Phys.* **A134** (1969) 505
- 16) P. W. M. Glaudemans and P. M. Endt, *Nucl. Phys.* **42** (1963) 367
- 17) A. J. Ferguson, *Angular correlation methods in gamma-ray spectroscopy* (North-Holland, Amsterdam, 1965)
- 18) P. B. Smith, in *Nuclear reactions II*, ed. P. M. Endt and P. B. Smith, (North-Holland, Amsterdam, 1962)
- 19) D. C. Camp and L. van Lehn, *Nucl. Instr.* **76** (1969) 192
- 20) H. Röpke and N. Anyas-Weiss, *Can. J. Phys.* **47** (1969) 1545
- 21) J. Kuperus, *Physica* **30** (1964) 2253
- 22) K. W. Carter, R. V. Elliott, D. C. Kean and R. H. Spear, *Nucl. Phys.* **A126** (1969) 49
- 23) V. F. Weisskopf, *Phys. Rev.* **83** (1951) 1073
- 24) C. van der Leun, *Proc. Kansas Symp. on the structure of low-medium mass nuclei* (Kansas, 1964) p. 109
- 25) C. van der Leun, D. M. Sheppard and P. M. Endt, *Nucl. Phys.* **A100** (1967) 316
- 26) G. M. Crawley, D. L. Powel and B. V. Narashima Rao, *Austral. J. Phys.* **21** (1968) 803
- 27) H. Röpke, (Freiburg) private communication (1971)